THE MULTI-FACTOR CONTROL AND EVALUATION OF HIGHWAY SOFT SOIL SUBGRADE STABILITY

Ming Zhang, Nan-nan Li and Min Yang

Henan University of Engineering, Institute of Civil Engineering, 1 Xianghe Road in Longhu, Xinzheng, Zhengzhou, China; mzhang@haue.edu.cn, 1511928525@qq.com, 2623169487@qq.com

ABSTRACT

When the surcharge preloading method is used in the treatment of soft soil subgrade, it is necessary to squeeze for more preloading drainage consolidation time under the premise of controlling the subgrade stability during the filling period. Considering the mutation of each monitoring indices and their interrelation when instability occurs in the fill subgrade, the inflection point analysis method through monitoring indices to control the subgrade stability comprehensively was proposed in this paper. The thin-layer rotary adding method was used to determine the ultimate filling depth and the loading plan for the highway soft soil subgrade during the filling period, with the inflection point analysis method in analyzing and evaluating the subgrade stability. The results showed that: (1) The ultimate fill height of the subgrade sections was obtained from the stability analysis results on the basis of the three indices of pore water pressure increment, settlement and lateral displacement, which was close to the prediction results of the thin-layer rotary adding method. (2) The stability control standard of the subgrade construction in the filling method was that the single-stage pore pressure coefficient should be within 1.2. (3) The subgrade stability control standard contained the maximum settlement rate of 20mm/d and the maximum lateral displacement rate of 3mm/d. (4) The geotextile setting in the highway subgrade effectively improved the ultimate bearing capacity of the subgrade, reduced the lateral displacement, improved the anti-slip stability, and increased the ultimate filling height and filling rate.

KEYWORDS

Soft soil subgrade, Stability, Ultimate filling height, Inflection point analysis, Thin-layer rotary adding method, Geotextile

INTRODUCTION

Deformation and stability control are the two major technical problems in the construction of high embankment highway [1], where the stability is the primary concern during the construction and filling period. Especially when constructing the highways in soft soil areas, due to the excessive fill speed and overfilling, and improper construction methods, once the foundation stability cannot be strictly controlled during the construction and filling period, the subgrade instability will occur. When constructing the high-grade highway on soft foundation such as silt, the surcharge preloading method is considered as a more economical and reasonable foundation treatment method. How to gain more time for the preloading drainage consolidation under the premise of controlling the subgrade stability during the construction and filling period, is a subject with great engineering and economic value.

The stability control methods for soft soil subgrade include both theoretical method and monitoring-based stability control. The theoretical method requires the accurate soil parameters, additionally, the application is limited by conditions. Rao Bo [2] considered the strength improvement of the soft soil with the growth of degree of consolidation, the effective consolidation

stress method was adopted in subgrade stability analysis, and according to the measured settlement, programmed to calculate the allowable filling height at any moment, which ensured the stability of the soft soil subgrade during filling construction period.

The stability control method based on monitoring usually used one or several observed empirical values as the control index of the subgrade stability, which is more intuitive and convenient. However, due to the different properties of the subgrade soil, loading method, loading rate and foundation treatment method, there are great differences between the quantitative control indexes of stability, leading to the obstacles in the stability control of soft soil subgrade construction. At present, the main monitoring items are the vertical settlement, lateral displacement and pore water pressure [3]. Many control methods for judging the stability of soft soil subgrade are put forward at home and abroad by the collation and analysis of these monitoring data. Tavenas et al. [4] defined the lateral deformation coefficient as the ratio of the filling rate Δq to the maximum lateral displacement rate ΔD_m at the toe of the embankment, and judged the stability of the embankment by establishing a relationship curve between $\Delta q/\Delta D_m$ and the embankment filling load q. Which verified this method is only effective for deep soft soil subgrade, but conservative. Brand and Brenner concluded that the stability discrimination method based on the pore water pressure increment $\sum\Delta U$ and cumulative filling load $\sum\Delta p$ ($\sum\Delta U\sim\sum\Delta p$) was more reasonable by studying on indoor and outdoor tests of soft clay [5]. However, when using this method, it is necessary to capture the peak value of excess pore water pressure in time and accurately, which is difficult for linear engineering such as highways. Ladd proposed the stability discrimination method on the basis of the lateral displacement and surface settlement [6]. Since the settlement caused by lateral displacement was a component of the surface settlement, consequently, when the lateral displacement changed abruptly, the surface settlement would also change, resulting in the hinder during the adoption of the method for stability discrimination. Because the lateral displacement test method cannot overcome the problems of inconsistent stiffness and deformation between soft soil and lateral displacement pipe, the accuracy of the test results remains to be further studied [7-10]. Huang Teng et al [11] proposed the stability discrimination method on the basis of measured settlement by combining the deformation and failure characteristics of soft clay, it could not only use the surface settlement information for stability discrimination, but also use the stratified settlement for stability discrimination of the weakest layer of the foundation. Wang Yanling [12] summarized three kinds stability control methods of high filled subgrades in soft soil areas, including the displacement rate method, the method of the ratio of maximum horizontal displacement and the settlement of the center of the subgrade, and the regression formula used in Japan. By analyzing an example, it is concluded that the ratio method was worthy of recommending method for the soft soil subgrade stability.

Wang Yanhui [13] used the settlement on daily filling to replace the undrained settlement, and proposed the grey system theory to generate cumulative treatment of the instantaneous settlement caused by each level of loading (AGO stability judgment method [14]) to estimate the stability of soft soil subgrade in mountainous areas. Although the method was simple and consistent with engineering practice, it was conservative.

Most scholars often took one field monitoring value as the control standard of soft soil subgrade stability, which was not comprehensive enough for the consideration of the monitoring and control standard of the stability, and the stability judgment was conservative in most cases. Before the instability failure of soft soil subgrade filling, the horizontal displacement and displacement rate of the subgrade slope foot, surface settlement at the subgrade center, stratified settlement, deep horizontal displacement, and excess pore water pressure would radically change. Therefore, when the above monitoring indexes were used as the stability control criteria for soft soil subgrades, the internal connection between them should be considered, and the comprehensive and multi-factor control method with multiple indexes simultaneously was adopted to evaluate the stability of soft soil subgrade.

In this paper, the thin-layer rotary adding method for the stability control and the loading plan determination for the soft soil subgrade during the filling period. Combined with the surcharge preloading method project in highway soft soil subgrade, using the thin-layer rotary adding method

to calculate the ultimate filling height and the loading plan, and applying the inflection point analysis method (often used for monitoring indexes to control the stability of subgrades in a comprehensive way) on the stability analysis and evaluation of soft soil subgrade during the filling period, providing a feasible method with both theory and practice for the stability control and evaluation of highway soft soil subgrade.

THEORETICAL CALCULATION METHOD FOR STABILITY OF SOFT SOIL SUBGRADE

Ultimate filling height

The limit filling height was the maximum filling height of the natural foundation under sliding failure by using the limit equilibrium theory, which was generally calculated by the circular sliding method. To determine the location and radius of the center of the most dangerous sliding surface in the circular sliding method was quite tedious in the stability analysis of soft soil subgrade, which usually required a computer to do multiple calculations. To facilitate the application, the ultimate filling height was calculated using the following Fellenius formula [15]:

$$H_f = \frac{C_u N_c}{k\gamma} \tag{1}$$

Where C_u was the vane shear strength, k was the safety factor, γ was the bulk density of subgrade filling, and N_c was the bearing capacity factor, generally taken as 5.52.

Determination of loading plan by thin-layer rotary adding method

Drainage consolidation method was an economical and reasonable method of foundation treatment for soft soil subgrades, and the reinforcement effect would be better if sufficient drainage consolidation time was given to soft soil subgrade under surcharge loads. After many years of practical engineering experience and testing results, an effective and practical method of load stopping-the thin-layer rotary adding method was proposed. This method required that the strength growth of the foundation soil after one paving and compaction could just reach the capacity of filling next layer. Taking advantage of the strength growth of the foundation soil to achieve the purpose of rapid filling the embankment [16]. The detailed steps were as follows:

(1)   Calculate the strength increase ΔC_{ui} in foundation soil required for the filling thickness Δh_i at level i. From Equation (1), we got:

$$\Delta C_{ui} = \frac{\gamma \cdot \Delta h_i \cdot k}{N_c} \tag{2}$$

(2)   Calculate the loading time t_n for any filling load at n level

Let t_1, t_2, …, t_n be the time applying the 1, 2 and n level filling loads respectively (starting from zero, and t0=0 at the beginning of loading), t_i' was the loading duration time at the i level load, and t_0' was the loading duration time at the initial filling load. $\Delta\sigma$ was the accumulated additional vertical stress when applying the n level of filling load, φ_{cu} was the consolidated fast shear internal friction angle of the foundation soil, and the weighted average value of each layer soil in the compression layer or the weakest layer of the foundation soil was selected as the control index. Δh_i and ΔP_i were the i level filling height and the corresponding load increment respectively, and Δh_0 and ΔP_0 were the ultimate filling height and the corresponding load increment respectively. U_t was the average degree of consolidation of foundation at instantaneous loading t, and U_t' was the average consolidation degree of foundation under the n-level constant speed loading at t time, calculated according to Equation (3).

$$U_t' = \sum_{i=1}^{n} (U_{t-\frac{t_i+t_{i-1}}{2}} \cdot \frac{\Delta P_i}{\sum \Delta P}) \tag{3}$$

Where t_{i-1} and t_i were the starting and ending times of the i-level load respectively. During each loading process, let $t_i=t$. And $\sum \Delta P$ was the summation of n levels load. According to the strength growth formula, $\Delta C_u = U_t \cdot \Delta \sigma \cdot tg\varphi_{cu}$. Considering the shear creep and the strength attenuation effect under shear stress and other factors, the reduction factor η should be multiplied (According to the measured results, η was taken from 0.8 to 0.85; If the foundation soil had no strength attenuation, η=1), we have:

$$\sum_{i=1}^{n}\Delta C_{ui} = \eta \cdot U'_t \cdot \Delta\sigma \cdot tg\varphi_{cu}$$

$$= \eta \cdot tg\varphi_{cu} \cdot \left(U_{t_n-t'_0/2} \cdot \Delta P_0 + U_{t_n-t_1-t'_1/2} \cdot \Delta P_1 + \cdots + U_{t_n-t_{n-1}-t'_{n-1}/2} \cdot \Delta P_{n-1} \right)$$

$$= \eta \cdot tg\varphi_{cu} \cdot \sum_{i=1}^{n}\left(U_{t_n-t_{i-1}-t'_{i-1}/2} \cdot \Delta P_{i-1} \right) = \eta \cdot tg\varphi_{cu} \cdot \sum_{i=1}^{n}\left\{ \Delta P_{i-1} \cdot \left[1-\alpha e^{-\beta(t_n-t_{i-1}-t'_{i-1}/2)} \right] \right\}$$

$$= \eta \cdot tg\varphi_{cu} \cdot \left\{ \sum_{i=1}^{n}\Delta P_{i-1} - \alpha \sum_{i=1}^{n}\left[\Delta P_{i-1} \cdot e^{-\beta t_n+\beta(t_{i-1}+t'_{i-1}/2)} \right] \right\}$$

$$= \eta \cdot tg\varphi_{cu} \cdot \left\{ \sum_{i=1}^{n}\Delta P_{i-1} - \alpha \cdot e^{-\beta t_n} \cdot \sum_{i=1}^{n}\left[\Delta P_{i-1} \cdot e^{\beta(t_{i-1}+t'_{i-1}/2)} \right] \right\} \tag{4}$$

After sorting, we can get:

$$e^{-\beta t_n} = \frac{\eta \cdot tg\varphi_{cu} \cdot \sum_{i=1}^{n}\Delta P_{i-1} - \sum_{i=1}^{n}\Delta C_{ui}}{\eta \cdot tg\varphi_{cu} \cdot \alpha \cdot \sum_{i=1}^{n}\left[\Delta P_{i-1} \cdot e^{\beta(t_{i-1}+t'_{i-1}/2)} \right]} \tag{5}$$

After solving, we obtained:

$$t_n = -\frac{1}{\beta} \cdot \ln\left\{ \frac{\eta \cdot tg\varphi_{cu} \cdot \sum_{i=1}^{n}\Delta P_{i-1} - \sum_{i=1}^{n}\Delta C_{ui}}{\eta \cdot tg\varphi_{cu} \cdot \alpha \cdot \sum_{i=1}^{n}\left[\Delta P_{i-1} \cdot e^{\beta(t_{i-1}+t'_{i-1}/2)} \right]} \right\} \tag{6}$$

If all loading were completed instantaneously, i.e., $t'_0 = t'_1 = t'_2 = \cdots = t'_{n-1} = 0$, Eq (6) could be simplified as:

$$t_n = -\frac{1}{\beta} \cdot \ln\left[\frac{\eta \cdot tg\varphi_{cu} \cdot \sum_{i=1}^{n}\Delta P_{i-1} - \sum_{i=1}^{n}\Delta C_{ui}}{\eta \cdot tg\varphi_{cu} \cdot \alpha \cdot \sum_{i=1}^{n}(\Delta P_{i-1} \cdot e^{\beta t_{i-1}})} \right] \tag{7}$$

Substituting Eq (2) into Eq (6), we could get:

$$t_n = -\frac{1}{\beta} \cdot \ln\left\{ \frac{N_c \cdot \eta \cdot tg\varphi_{cu} \cdot \sum_{i=1}^{n}\Delta h_{i-1} - k \cdot \sum_{i=1}^{n}\Delta h_i}{N_c \cdot \eta \cdot tg\varphi_{cu} \cdot \alpha \cdot \sum_{i=1}^{n}\left[\Delta h_{i-1} \cdot e^{\beta(t_{i-1}+t'_{i-1}/2)} \right]} \right\} \tag{8}$$

Where α, β were adopted according to the drainage and consolidation conditions of foundation soil in accordance with Table 5.2.7 of Technical Specification for Building Foundation Treatment JGJ 79-2012 [17].

THE CONTROL METHOD OF SUBGRADE STABILITY

Apparent characteristics of foundation instability

There were usually some premonitions before the instability failure occurred in the subgrade, which mainly as followed [18]: (1) some microcracks appeared on the top of loading, slope site and slope surface; (2) ground uplift near the loading slope site; (3) the surface settlement, deep horizontal displacement and pore water pressure in the loading area increased sharply; (4) continued development of longitudinal cracks with circular shape after stopping loading; (5) continued increase in ground uplift near the loading slope site after stopping loading;

(6) continued increase in various monitoring indexes or insignificant convergence after stopping loading.

Inflection point analysis method on the basis of monitoring

In actual construction, the appearance of apparent characteristics does not necessarily represent the instability of subgrade. When one of the settlement rate, lateral displacement rate and pore water pressure coefficient during loading exceeds the quantitative control index, the foundation is not destabilized, and it is necessary to evaluate the stability of soft soil subgrade through the comprehensive analysis with the above monitoring data. Staged filling of soft soil subgrade with the thin-layer intermittently adding method, the two-level filling interval is about seven days, and each level filling is completed within one day. The loading rate far exceeds the dissipation rate of pore water pressure in the soil, which formed the effect of undrained shear. And the response of pore water pressure of embankment soft soil unit under undrained condition is divided into following three stages (as shown in Figure 1).
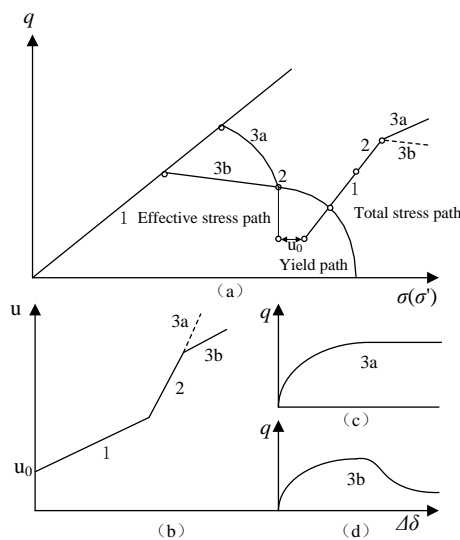
Fig. 1 – Stress path of the soft soil element of subgrade
(a) Stress path in the site; (b) The relationship between pore water pressure u and shear deformation $\Delta\delta$;
(c) Hardening phenomenon; (d) Softening phenomenon

(1)   Elastic stage. At this stage, part of the additional stress is borne by the pore water due to the influence of soil structure, namely $\Delta u < \Delta\sigma_z$. The relationship between the pore water pressure increment and load increment at one subgrade soil point under large preloading load is given by $\Delta u = B\Delta p$, where B is the pore pressure coefficient and $B<1$, as shown in the stress path in curve 1 in Figure 1.

(2)   Plastic stage. At this stage, as the external load increase, the shear stress in soil exceeds the shear strength between the soil particles, the bond between the soil particles breaks down, and the structure readjusts and begins to produce plastic deformation. Then the additional stress is basically borne by the pore water pressure, namely $\Delta u \approx \Delta\sigma_z$, and shear instability occurs locally in the subgrade, as shown in the stress path in curve 2 in Figure 1.

(3)   Hardening or softening stage. At this stage, after the connection failure between the soil particles, the soil particles position moves, accompanied by the increase of plastic deformation. Due to the soil structural characteristics, the deformation of soil will be bifurcation. In one case, the arrangement between soil particles tends to a more stable state, with the so-called hardening phenomenon (Figure 1(c)) and the stress path shown in curve 3a in Figure 1; in the other case, the softening phenomenon (Figure 1(d)) occurs as the failure point of the soil increases, with the stress path shown in curve 3b in Figure 1.

From the above analysis, it could be shown that the key is the appearance of the plastic deformation stage, that is, the appearance of the first inflection point in $\Delta u \sim \Delta p$ curve, indicating that local shear failure has happened in the soil where the pore gauge is located. And if inflection points appeared in all the pore gauge at different depths, showing that the foundation is in a state of overall instability.

ENGINEERING EXAMPLE ANALYSIS

Test section overview

The first phase of Guangzhou-Zhuhai Expressway starts from Guangzhou in the north to Hainan Village in the south and ends at Bijiang, Beijiao Town, Shunde City, with a total length of 14.659km. The route is located in the alluvial plain of the Pearl River Delta, and the distribution of soft soils is extremely uneven, with a general thickness of 1 to 5m and local sections exceeding 10m. The main road section is the intersection of bridges and soft foundations, with thicker soft soil layers and higher embankment fill, problems of embankment stability and uneven settlement at the connection between bridge head and embankment are obvious. At the same time, the influence of lateral pressure generated by high fill on the embankment cannot be ignored, especially the abutment pile foundation of the that intersects the route diagonally, if not handled properly, the stability and safety of the embankment would be affected. Combined with local experience, proposing surcharge preloading method on soft foundation treatment, and a small amount of geotextile reinforcement is set in some soft soil and high fill sections to establish a soft soil foundation monitoring system, in accordance with the thin-layer rotary adding method for subgrade filling construction. The section from K11+021 to K11+220, where the thickness of silt layer is 13.5 m and the height of fill is large (maximum 7.2m, minimum 6m), was selected for soft foundation test. According to the geological conditions and design data of the test section, the test arrangement of geotextiles is shown in Table 1, the arrangement of monitoring and monitoring instruments is shown in Table 2, and the arrangement of the buried cross-sectional of monitoring and monitoring instruments is shown in Figure 2.

Tab. 1: Test Arrangement of Geotextiles

Pile no.	Original design scheme	Safety coefficient of subgrade stability	Test scheme	Remark
K11+021~K11+070	Three-layer geogrid	1.213	Two-layer geotextile	Equal load
K11+070~K11+166	Two-layer geogrid	1.259	One-layer geotextile	Surcharge
K11+166~K11+220			No geotextile	Surcharge

Tab. 2: Arrangement of Monitoring and Monitoring Instruments

Section	Inclinometer tube	Pore water pressure gauge	Earth pressure	Layered settlement hole	Surface settlement
K11+032	One hole (15m)	One hole (Three gauges)			
K11+045	One hole (15m)	One hole (Three gauges)	Three		Three
K11+116	One hole (15m)	One hole (Five gauges)	Three	One hole (15m)	Five
K11+166		One hole (Four gauges)			Three
K11+196	One hole (15m)	One hole (Five gauges)		One hole (15m)	Three
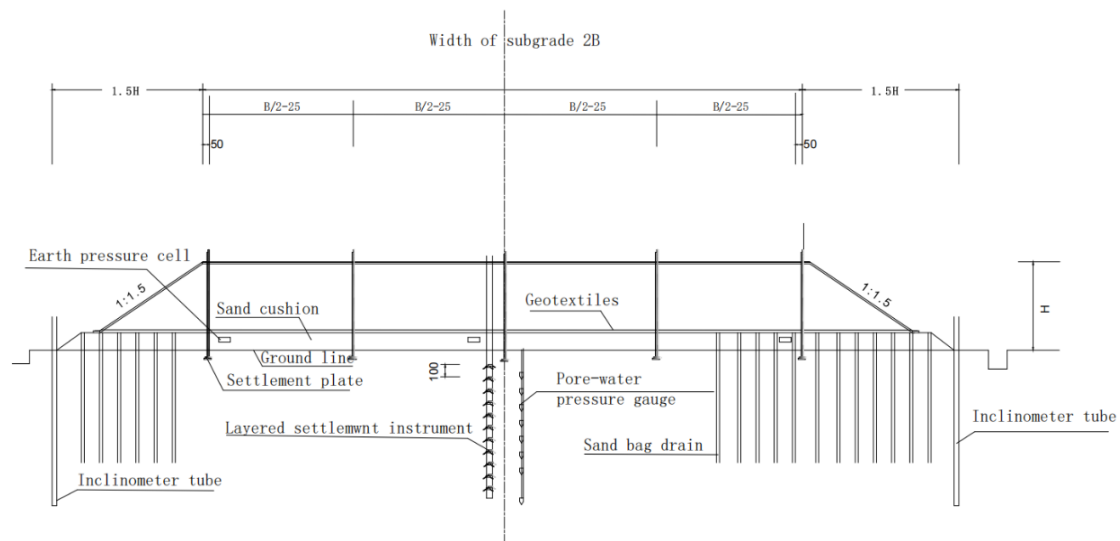
Fig. 2 – The cross-sectional schematic diagram of the buried monitoring instruments

Ultimate filling height

Due to the soil disturbance during the construction of bagged sand wells, reducing the soil strength. When the ultimate filling height was calculated with Eq. (1), the soil strength should be taken as the strength after construction disturbance. According to the test results of soft soil foundation of several highways in the region, the construction disturbance reduced the strength of surrounding soil by about 45%, and the ultimate filling height of each section of subgrade was calculated according to this strength loss, as shown in Table 3.

Tab. 3: Ultimate Filling Height of Each Subgrade Section

Section	γ /(kN/m³)	Cu/kPa		k_{min}	H_f /m
		Initial value	Calculation value considering strength loss		
K11+045	19	13.34	7.34	1.0	2.0
K11+084	19	12.08	6.64	1.0	1.9
K11+116	19	12.71	6.99	1.0	1.9
K11+166	19	14.60	8.03	1.0	2.2
K11+196	19	16.80	9.24	1.0	2.6

Loading plan

According to the main calculation parameters of each section shown in Table 4, the loading plan of the corresponding section was obtained from Eq (8), as shown in Table 5. In Table 4, the sand drains were arranged in squares with spacing of 1.2m, and the treatment depth of K11+045 subgrade section was 13m and 12m for the other sections, with the height H from the bottom of soft soil layer to the ground.

Tab. 4: Main Calculation Parameters of Each Subgrade Section

Section	$\varphi_{cu}/\,(°)$	$C_v/(10^{-3}cm^2/s)$	$C_r/(10^{-3}cm^2/s)$	H/m	$\beta_v/(10^{-7}s^{-1})$	$\beta_r/(10^{-7}s^{-1})$
K11+045	12.8	8.5	1.25	12.5	0.134	2.930
K11+084	12.9		1.15	8.8		2.695
K11+116	11.7		1.33	10.2		3.117
K11+166	14.6	9.0	0.86	12.4	0.144	2.016
K11+196	11.3	8.5	1.035	9.7	0.229	2.426

Tab. 5: Loading Plan of Each Subgrade Section

Section	Ultimate filling soil		Planned filling height /m	Planned filling height per level /m	Average loading time per level /d		Duration time of loading to design load /d
	Height /m	Loading duration time /d			Loading duration time	Intermittent time	
K11+045	3.2	10	10.8	0.25	1	4	145
				0.45	2	7	157
				0.65	2	11	169
K11+084	2.2	10	8.1	0.25	1	7	190
				0.45	2	13	199
				0.65	2	21	216
K11+116	2.2	10	7.8	0.25	1	9	243
				0.45	2	20	293
				0.65	2	45	437
K11+166	2.5	10	8.1	0.25	1	5	148
				0.45	2	9	157
				0.65	2	15	164
K11+196	2.5	10	7.5	0.25	1	9	215
				0.45	2	18	233
				0.65	2	34	295

Subgrade stability analysis

In order to comparative analysis, the pore water pressure increment $\Delta u_{7.5}$, single-stage pore pressure coefficient B (taking the middle of the soft soil layer), cumulative settlement S and lateral displacement rate V_c for K11+045, K11+166 and K11+196 subgrade sections are summarized in supplementary Tables 1 to 3. The cumulative filling height in the tables ignored the settlement value, which was considered in the actual cumulative filling height. The data in the tables were the observation data before the filling soil of the next layer, and the last layer of filling data was the data of 7 days after filling. $\Delta u_{7.5}$ in the tables indicated the pore water pressure increment of the pore gauge at the burial depth of 7.5m, $\delta_{7.0}$ indicated the cumulative lateral displacement at the burial depth of 7.0m, and the rest was the same. The relationship between these monitoring data and load could be used to determine the subgrade stability and reasonable loading time.

Analysis on the increment of pore water pressure

The relationship curves between the cumulative pore water pressure increment $\sum\triangle u$ and cumulative load $\sum\triangle P$ were obtained with the data in supplementary Tables 1 to 3, as shown in Figure 3. It could be seen from Figure 3 that the curve of $\sum\triangle u\sim\sum\triangle P$ for each section was approximately linear at initial loading stage, and the tangent slope of the curves decreased at the later loading stage, indicating that the cumulative pore water pressure increment decreased at the later loading stage, the consolidation degree of foundation increased, the strength increased, and the deformation tended to be stable. Figure 3 depicted that the turning points emerged in the

∑△u~∑△P curves during the loading period throughout the filling period. In Figure 3, at the section K11+045, the first turning point occurred at the fourth level filling load (corresponding to the filling height of 3.286m), namely, the curve was basically linear at the filling height of 3.286m, and when the next level of filling load (corresponding to the filling height of 3.799m) was to be filled again, the curve bended upward and the slope increased. According to the elastic-plastic theory of soil, the soil entered the plastic deformation stage when the filling height increased from 3.286m to 3.799m. Therefore, the filling height corresponding to the transformation of the section soil from elastic to plastic stage could be taken as the average value of 3.543m, which was close to the ultimate filling height calculated theoretically. Similarly, the filling heights corresponding to the transformation of the section K11+166 and K11+196 soil from elastic to plastic stage were 2.854m and 2.61m respectively, which were also close to the ultimate filling heights calculated theoretically.
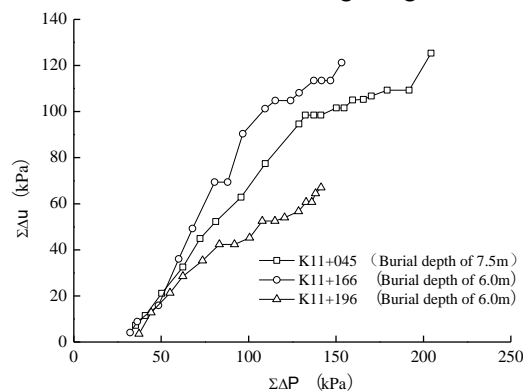
Fig. 3 – The relationship curve between ∑△u and ∑△P of each section

It could be seen from Figure 3 that when each section was loaded at the last two levels loading, the upward turning points emerged in the ∑△u~∑△P curves of each section, which was mainly because the loading rate is too fast, and the soil could not be consolidated by drainage, forming a fast-undrained shear state and making the soil instability. After taking the measures to stopping loading or unloading, the slope of the curve became smaller and the foundation tended to be stable.

The above analysis showed that within the ultimate filling height, ∑△u~∑△P curve was linear and the foundation soil was in elastic stage, at this time, the loading rate could be accelerated. After exceeding the ultimate filling height, an upward inflection point appeared in the ∑△u~∑△P curve, and the soil was in the plastic deformation stage. At this time, the loading speed should be slowed down, and the loading could continue until it reached the required consolidation degree. During the loading process, when the upward turning point emerged in the ∑△u~∑△P curve, indicating increasing the tangent slope of the curve, the foundation was unstable and should be stopped or unloaded immediately.

The relationship curves between the single-stage pore pressure coefficient B and cumulative load ∑△P were obtained with the data in supplementary Tables 1 to 3, as shown in Figure 4. Figure 4 and supplementary Tables 1 to 3 demonstrated that some of the single-stage pore pressure coefficients B exceeded the loading control standard of 1.0, but the subgrade soil was not instability. Which was mainly because the test section was constructed by the blowing filling method, and the sand contained a large amount of water, with the effect of power equipment, the ratio between the increment of excess pore water pressure and load increment was larger than the calculated value. And the single-stage pore pressure coefficient B exceeded 1.2 at the inflection point of the ∑△u~∑△P curve in all three sections. When adopting the blowing filling method, it is recommended that the single-stage pore pressure coefficient B control standard was smaller than 1.2.
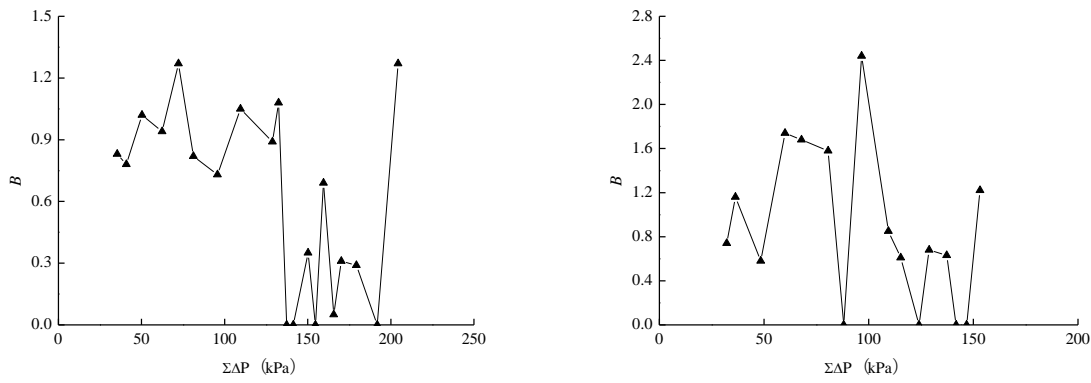
(a) Burial depth of 7.5m at the section K11+045   *(b) Burial depth of 6.0m at the section K11+166*
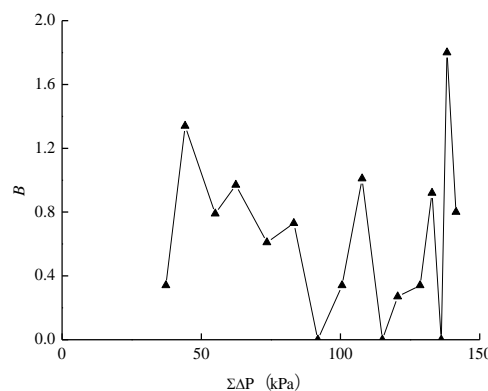
(c) Burial depth of 6.0m at the section K11+196

Fig. 4 – The relationship curve between B and $\sum\triangle P$ of each section

In Figure 3, taking the section K11+045 as the example to analyze the loading interval time. When the filling height increased from 0 to 3.286m (close to the ultimate filling height), it took 102 days, with an average of 32.2mm per day, including 40cm to 60cm of each loading height. When the filling height increased from 3.286m to 6.97m, it took 191 days, with an average of 19.3mm per day, including 50cm to 70cm of each loading. And when the filling height increased from 6.97m to 9.433m, it took 62 days, with an average of 39.7mm per day, which was close to the filling rate before the ultimate fill height. The average filling rate was 39.7mm per day for 62 days from 6.97m to 9.433m, which was close to the filling rate before the ultimate filling height, including 20cm to 30cm of each loading height. The above analysis showed that when proposing the thin-layer rotary adding method for loading, thinner the load of each layer would lead to the faster consolidation of the foundation, the faster the loading rate is, and the more stable foundation, which was consistent with the theoretical analysis results of the thin-layer rotary adding method using the foundation strength growth to guide the loading, indicating that adopting the thin-layer rotary adding method in guiding the filling construction was feasible both theoretically and practically.

Settlement analysis

The relationship curves between the cumulative settlement rate $\sum V$ and cumulative filling height $\sum \Delta h$ was obtained with the data in supplementary Tables 1 to 3, as shown in Figure 5. Figure 5 showed that the curve was a linear relationship in the steady state of the foundation. Excessive filling rate would lead to the larger soil shear deformation, significant increase of the settlement, and significant increase of the loading rate of the level. And an upward inflection point emerged in the curve, namely, the slope of the curve increased, indicating that the subgrade was at risk of instability. At this time, the observation of lateral displacement and pore water pressure should be strengthened, and measures such as stopping loading and unloading should be taken when necessary. which was consistent with the analysis results of the $\sum\triangle u \sim \sum\triangle P$ curve.
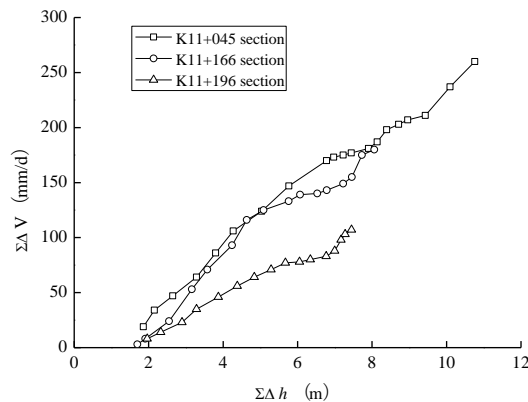
Fig. 5 – The relationship curve between ∑V and ∑△h of each section

From supplementary Tables 1 to 3, it can be seen that when the $\sum\triangle u \sim \sum\triangle P$ curve of K11+045 and K11+166 sections appeared the upward inflection point, the corresponding settlement rates exceeded 20mm/d (the maximum is 29mm/d). When the settlement rate was less than 20mm/d, no upward inflection point appeared. However, the settlement rate of K11+196 section during the whole loading process was small, which is less than 12mm/d. To make it clear, the fast settlement rate could not indicate the immediate instability of the foundation, but through observing the change of lateral displacement and judging whether the settlement was mainly caused by the undrained shear deformation under the current load. If the lateral displacement or lateral displacement rate increased too fast, it indicated that the foundation would be at risk of instability. Otherwise, the excessive settlement could only be explained by the consolidation settlement under the previous levels filling load or the insufficient foundation bearing capacity under the current level filling loading. The former would lead to the increase of foundation strength and the foundation tend to be stable, and the latter would lead to the soil to enter the plastic deformation stage from the elastic stage, prompting the consolidation of the foundation. Therefore, When the surface settlement rate was used as the standard to control the loading rate, the settlement rate should be greater than 20mm/d. However, the surface settlement rate was only regarded as a reference standard, and the horizontal lateral displacement was used as the main control standard.

Lateral displacement analysis

The relationship curve between the cumulative lateral displacement rate $\sum Vc$ and cumulative filling height $\sum\Delta h$ was obtained with the data in supplementary Tables 1 to 3, as shown in Figure 6. It could be seen from Figure 6 that the upward inflection point appeared in the curve of each section at the last two levels of filling. The slope of the curve increased and the growth of the lateral displacement rate accelerated. This is mainly due to the rapid filling, and the maximum lateral displacement rate reached 8.75mm/d. According to supplementary Tables 1 to 3, when the lateral displacement rate was close to 3mm/d, the upward inflection point in the curve showed up, consequently, the control standard of the lateral displacement rate was 3mm/d.

The relationship curve between the cumulative lateral extrusion V_h, the cumulative lateral displacement $\delta_{7.0}$ and cumulative filling height $\sum\Delta h$ were obtained with the data in supplementary Tables 1 to 3, as shown in Figure 7 and Figure 8. It could be seen from Figure 7 and Figure 8 that if the filling rate was too fast, the shear deformation of the soil increased, the accumulated lateral extrusion V_h and the accumulated lateral displacement $\delta_{7.0}$ increased significantly, and the appearance of the upward inflection point in the curve, namely, increasing the slope of the curve, indicating that the subgrade would become instability, measures such as stopping load and unloading should be taken at this time, which was consistent with the analysis results of the

previous $\sum\triangle u \sim \sum\triangle P$ curve.
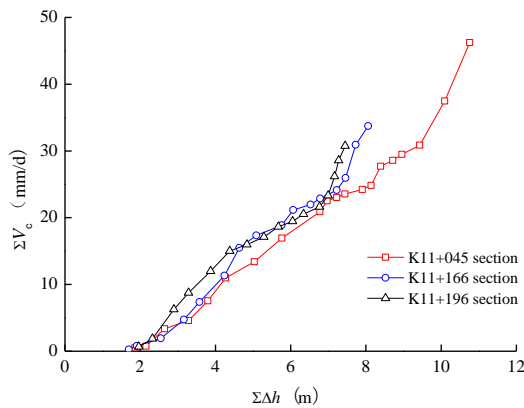
Fig. 6 – The relationship curve between ∑V_c and ∑△h of each section
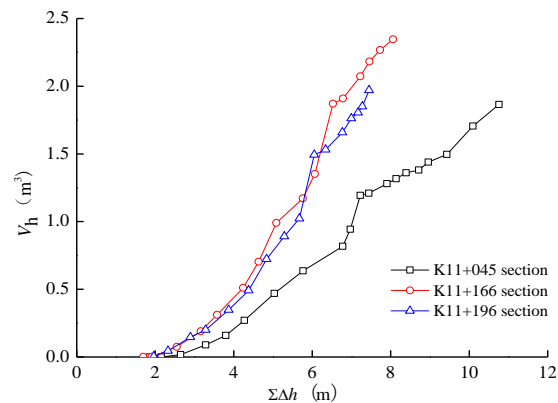
Fig. 7– The relationship curve between V_h and ∑△h of each section
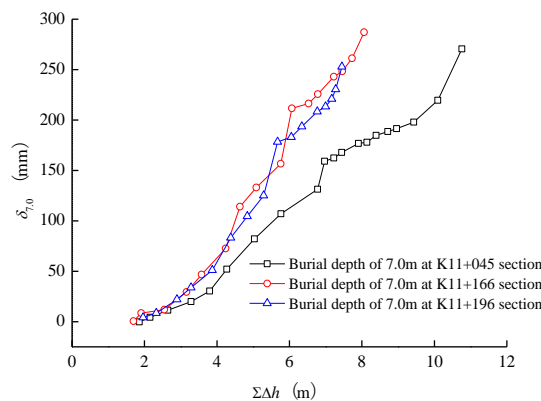
Fig. 8 – The relationship curve between δ$_{7.0}$ and ∑△h of each section

Within the ultimate filling height, the soil was in the elastic deformation stage, the curve was straight. When the filling height exceeded the ultimate filling height, the soil would enter the plastic deformation stage from elasticity, the lateral displacement rate, lateral extrusion, lateral displacement would increase significantly, the slope of the curve increased, and then the first upward inflection point appeared. Consequently, the ultimate filling height could be approximately determined according to the first upward inflection point of the curve. As shown in Figures. 6-8, there was an upward inflection point of K11+045 section when the filling height reached 3.286m, namely, when the filling height increased from 3.286m to 3.799m, the soil properties changed from the elastic stage to the plastic deformation stage, and the ultimate filling height of K11+045 section could be approximately determined as 3.543m. Similarly, the ultimate filling heights of K11+166 and K11+196 sections could be determined as 2.854m and 2.61m respectively, which were consistent with the analysis results of the previous ∑△u~∑△P curves.

Reinforcing effect of geotextiles

The geotextile was often used to improve the anti-sliding stability of subgrade and increase the ultimate filling height. The comparisons of the theoretical ultimate fill height of each subgrade section and the results of analysis through monitoring data were shown in Table 6. The one layer geotextile and two layers geotextile increased the ultimate filling height by 0.65m and 1.55m respectively, accordingly, the geotextile had a greater effect on improving the anti-sliding stability of the foundation and speeding up the filling rate of the subgrade.

Tab. 6: Comparison between the Theoretical Calculation of Ultimate Filling Height and the Analysis Results of Monitoring Data

Section	Theoretical calculation of ultimate filling height A/m	Analysis results of ultimate filling height by the monitoring data C /m	C-A /m	Remarks
K11+045	2.0	3.543	1.543	Two layers geotextile
K11+166	2.2	2.854	0.654	One layer geotextile
K11+196	2.6	2.61	0.01	no geotextile

The comparison curves of $\sum V_c \sim \sum \Delta V$, $\delta_{7.0} \sim S$, $V_h \sim S$ and $\delta_{7.0}/S \sim S$ of each section were obtained with the data in supplementary Tables 1 to 3, as shown in Figure 9. It could be seen from Figure 9 that the curve of section K11+045 was at the bottom, the curve of section K11+196 was at the top, while the curves of section K11+166 was in the middle, indicating that the geotextile could effectively constrain the lateral displacement and lateral extrusion, reduce the final settlement of the foundation and increase the anti-sliding stability of the foundation.

(a)

(b)

(c)

(d)
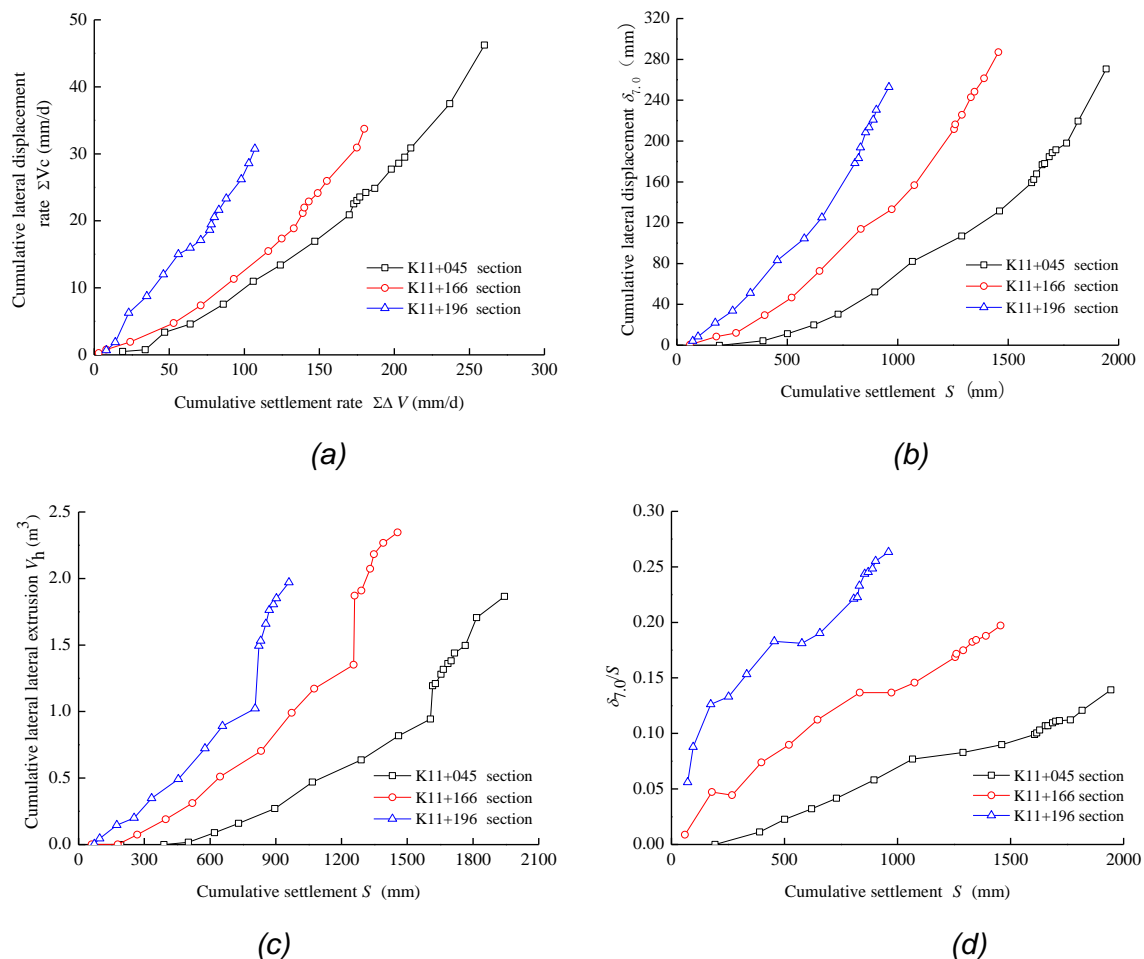
Fig. 9 – The comparison curves of $\sum V_c \sim \sum \Delta V$, $\delta_{7.0} \sim S$, $V_h \sim S$ and $\delta_{7.0}/S \sim S$ of each section

When the geotextile was set in the subgrade soil, due to the effect of friction between the geotextile and the subgrade soil, the tensile stress in the soil was transferred to the geotextile. Therefore, the geotextile was under tensile stress, and the subgrade soil was under compressive stress and shearing stress between geotextiles. The geotextile and subgrade soil could live up to their potential, so the cohesion effect and the built-in function between the geotextile reinforced body and the soil had generated, which could enhance the integrity and continuity of soil, limit the lateral displacement of soil and increase the stability of subgrade.

In addition, due to the stress diffusion effect of the geotextile, the additional stress of the subgrade soil under the geotextile decreased, so that the vertical compression deformation of soil decreased. Because the geotextile was subjected to tensile stress, the tensile stress was balanced by the interface shear stress. Under the action of the interface shear stress, the subgrade soil produced uplift deformation, which could offset the partial settlement of the subgrade, reduce the final settlement of the subgrade and increase the stability of the subgrade.

Comprehensive comparative analysis

Through the comprehensive comparative analysis of Figures 3 to 6, the internal relations between them was analyzed. In Figure 3 (section K11+045), the curve was basically straight during the first four levels load (corresponding to the filling height of 3.286 m), and then the slope of the curve increased slightly from the fifth level load (corresponding to the filling height of 3.799 m). The corresponding settlement rate of the section K11+045 in Fig 5 increased slightly and the lateral displacement rate of the section K11+045 In Figure 6 also increased obviously, with an upward inflection point, indicating that the local shear failure of the soil began to occur, and then the part of the soil continued to undergo shear failure, and began to harden, consolidation, and the slope of the curve gradually decreased. After maintaining a straight section, and the foundation strength gradually increased and the subgrade tended to stabilize. The same results could be obtained from the curve analysis of other sections, indicating that the $\sum \triangle u$ to $\sum \triangle P$ curve, $\sum \triangle V$ to $\sum \triangle h$ curve and $\sum V_c$ to $\sum \triangle h$ curves were consistent. At the same time, the lateral displacement rate was highly sensitive to the foundation state. Therefore, in the monitoring process of soft soil subgrade, the lateral displacement and displacement rate should be used as the main monitoring indexes, which were the important indicators to determine whether the foundation was stable.

When drawing the curves of $\sum \triangle V \sim \sum \triangle h$ and $\sum V_c \sim \sum \triangle h$, the attention should be paid to the treatment of load levels. Because the daily settlement or lateral displacement of the filling load at this level contained the daily consolidation deformation under the previous levels filling load and the undrained shear deformation produced by the filling load at this level. When the loads at all levels were similar and the loading interval time was similar, the curve could basically eliminate the influence of the daily consolidation deformation under the previous levels filling loads, and the slope of the curve could reflect the change direction of the undrained shear deformation produced by the filling load at the corresponding level. If a certain level load is very small, comparing the daily consolidation deformation under the previous levels filling loading and the undrained shear deformation produced by this level filling load, the increasing of the former proportion, would result in a larger slope of the curve. while the surface settlement and lateral displacement rate may not actually increase. Therefore, when the load was small, it could be combined with the previous levels load into the first level load, and the slope of the curve was comparable. Similarly, the unloaded load should be treated as the previous level load when unloading, otherwise the curve would be reversed.

CONCLUSION

(1)   Drainage consolidation method was always used to treat soft soil subgrade, and the thin-layer rotary adding method was proposed to determine the loading plan and the ultimate filling height to control the graded surcharge thickness, which was a practical method to effectively control subgrade stability both in theory and practice.

(2)   According to the soil failure theory and the pore water pressure response generated by the graded filling subgrade with the thin-layer rotary adding method, the deformation of soft soil subgrade was divided into the elastic stage, plastic stage, hardening or softening stage, and the inflection point analysis method based on monitoring was proposed to evaluate the stability state of soft soil subgrade.

(3)   The proposed stability calculation theory and control method were applied on the comprehensive analysis of the monitoring data of the test section of soft soil subgrade in the

highway to evaluate the stability of soft soil subgrade. The results showed that: 1) When the inflection point appeared in the $\sum\triangle u \sim \sum\triangle P$ curve, that is, the slope increased, the soft soil subgrade was near to instability, and the subgrade monitoring should be strengthen. When the blow-filling method was used for the subgrade construction, the stability control standard was that the single-stage pore pressure coefficient B should be controlled within 1.2 during loading. 2) When no upward inflection point emerged in the $\sum\triangle V \sim \sum\triangle h$ and $\sum V_c \sim \sum\triangle h$ curves, the soft soil subgrade was stable. When an upward inflection point appeared in the curve, the soft soil subgrade was close to instability, so the monitoring of the change trend of the lateral displacement rate should be strengthened. If the lateral displacement rate continued to increase, and the subgrade was close to instability, measures such stopping load or unloading should be taken. 3) The control standard of soft soil subgrade stability was the maximum settlement rate was controlled within 20mm/d, and the maximum lateral displacement rate was controlled within 3mm/d.

(4)   Theoretical calculations and monitoring results showed that the geotextiles was able to effectively improve the ultimate bearing capacity of the subgrade soil, reduce lateral displacement, improve the anti-sliding stability of the subgrade, and accelerate the filling rate.

Appendix

Tab. 1: Monitoring Data of K11+045 Section

Calculation value of cumulative filling height(m)	Actual cumulative filling height $\sum\triangle h$(m)	Actual cumulative load $\sum\triangle P$ (kPa)	Lateral displacement rate V_c (mm/d)	Cumulative lateral displacement rate $\sum Vc$ (mm/d)	Cumulative lateral extrusion V_h (m³)	Maximum settlement rate V(mm/d)	Cumulative settlement rate $\sum V$ (mm/d)	Cumulative lateral displacement $\delta_{7.0}$ (mm)	Cumulative settlement S(mm)	B	$\triangle u_{7.5}$ (kPa)	$\sum\triangle u_{7.5}$ (kPa)
1.785	1.860	35.34	0.490	0.490	0	19	19	-0.22	193	0.83	7.2	7.2
1.959	2.152	40.89	0.260	0.750	0	15	34	4.35	390	0.78	4.3	11.5
2.255	2.645	50.26	2.610	3.360	0.0176	13	47	11.32	501	1.02	9.6	21.1
2.785	3.286	62.43	1.220	4.580	0.089	17	64	19.90	620	0.94	11.4	32.5
3.179	3.799	72.18	2.960	7.540	0.16	22	86	30.31	730	1.27	12.4	44.9
3.544	4.274	81.21	3.440	10.980	0.271	20	106	52.07	896	0.82	7.4	52.3
4.138	5.034	95.65	2.430	13.410	0.469	18	124	82.10	1067	0.73	10.5	62.8
4.699	5.766	109.55	3.540	16.950	0.636	23	147	106.92	1290	1.05	14.6	77.4
5.490	6.780	128.82	3.950	20.900	0.817	23	170	131.39	1461	0.89	17.2	94.6
5.509	6.970	132.43	1.620	22.520	0.943	3	173	159.08	1606	1.08	3.9	98.5
5.621	7.227	137.31	0.500	23.020	1.194	2	175	162.40	1616	0.00		98.5
5.825	7.441	141.38	0.530	23.550	1.21	2	177	167.79	1629	0.00		98.5
6.278	7.907	150.23	0.670	24.220	1.28	4	181	176.69	1654	0.35	3.1	101.6
6.482	8.136	154.58	0.610	24.830	1.317	6	187	177.90	1665	0.00		101.6
6.730	8.395	159.51	2.890	27.720	1.361	11	198	184.69	1686	0.69	3.4	105.0
7.031	8.717	165.62	0.860	28.580	1.381	5	203	188.64	1700	0.05	0.3	105.3
7.257	8.957	170.18	0.910	29.490	1.439	4	207	191.36	1716	0.31	1.4	106.7
7.717	9.433	179.23	1.370	30.860	1.497	4	211	197.95	1765	0.29	2.6	109.3
8.330	10.095	191.81	6.610	37.470	1.705	26	237	219.49	1817	0.00		109.3
8.941	10.758	204.40	8.750	46.220	1.865	23	260	270.55	1944	1.27	16.0	125.3

Tab. 2: Monitoring Data of K11+166 Section

Calculation value of cumulative filling height(m) $\sum\triangle h$(m)	Actual cumulative filling height $\sum\triangle h$(m)	Actual cumulative load $\sum\triangle P$ (kPa)	Lateral displacement rate V_c (mm/d)	Cumulative lateral displacement rate $\sum Vc$ (mm/d)	Cumulative lateral extrusion V_h (m³)	Maximum settlement rate V(mm/d)	Cumulative settlement rate $\sum V$ (mm/d)	Cumulative lateral displacement $\delta_{7.0}$ (mm)	Cumulative settlement S(mm)	B	$\triangle u_{7.5}$ (kPa)	$\sum\triangle u_{7.5}$ (kPa)
1.651	1.695	32.21	0.26	0.26	0.0015	3	3	0.53	60	0.74	4.09	4.09
1.850	1.910	36.29	0.52	0.78	0.002	5	8	8.45	179	1.16	4.72	8.81
2.370	2.549	48.43	1.14	1.92	0.074	16	24	11.90	268	0.58	7.06	15.87
2.891	3.159	60.02	2.82	4.74	0.1904	29	53	29.44	398	1.74	20.16	36.03
3.176	3.574	67.91	2.64	7.38	0.3109	18	71	46.60	520	1.68	13.22	49.25
3.722	4.242	80.60	3.94	11.32	0.51	22	93	72.61	646	1.58	20.10	69.35
3.988	4.634	88.05	4.16	15.48	0.704	23	116	113.93	833	0.00		69.35
4.254	5.087	96.65	1.87	17.35	0.9905	9	125	133.06	973	2.44	21.00	90.35
4.786	5.759	109.42	1.51	18.86	1.1714	8	133	156.66	1075	0.85	10.88	101.23
4.992	6.067	115.27	2.29	21.15	1.351	6	139	211.63	1255	0.61	3.56	104.79
5.272	6.527	124.01	0.82	21.97	1.8707	1	140	216.24	1260	0.00		104.79
5.526	6.786	128.93	0.92	22.89	1.9087	3	143	225.67	1291	0.68	3.36	108.15
5.935	7.226	137.29	1.26	24.15	2.0724	6	149	242.86	1331	0.63	5.29	113.44
6.130	7.461	141.76	1.81	25.96	2.183	6	155	248.30	1348	0.00		113.44
6.378	7.726	146.79	4.96	30.92	2.267	20	175	261.30	1391	0.00		113.44
6.671	8.062	153.18	2.80	33.72	2.346	5	180	287.04	1456	1.22	7.82	121.26

Tab. 3: Monitoring Data of K11+196 Section

Calculation value of cumulative filling	Actual cumulative filling height	Actual cumulative load $\sum\triangle P$ (kPa)	Lateral displacement rate V_c (mm/d)	Cumulative lateral displacement rate $\sum Vc$	Cumulative lateral extrusion V_h (m³)	Maximum settlement rate V(mm/d)	Cumulative settlement rate $\sum V$	Cumulative lateral displacement $\delta_{7.0}$	Cumulative settlement S(mm)	B	$\triangle u_{7.5}$ (kPa)	$\sum\triangle u_{7.5}$ (kPa)
1.933	1.962	37.28	0.66	0.66	0.004	8	8	4.03	72	0.34	3.55	3.55
2.253	2.325	44.18	1.21	1.87	0.045	6	14	8.42	96	1.34	9.21	12.76
2.801	2.897	55.04	4.38	6.25	0.146	9	23	21.97	174	0.79	8.56	21.32
3.110	3.284	62.40	2.51	8.76	0.201	12	35	33.67	253	0.97	7.15	28.47
3.620	3.873	73.59	3.23	11.99	0.348	11	46	51.06	333	0.61	6.87	35.34
4.049	4.382	83.26	3.03	15.02	0.491	10	56	83.19	455	0.73	7.02	42.36
4.382	4.837	91.90	0.94	15.96	0.723	8	64	104.48	577	0.00		42.36
4.714	5.291	100.53	1.15	17.11	0.891	7	71	125.01	657	0.34	2.90	45.26
5.015	5.672	107.77	1.54	18.65	1.023	6	77	178.30	806	1.01	7.28	52.54
5.248	6.054	115.03	0.82	19.47	1.494	1	78	183.12	823	0.00		52.54
5.522	6.345	120.56	1.07	20.54	1.531	2	80	193.52	831	0.27	1.47	54.01
5.937	6.768	128.59	1.07	21.61	1.659	3	83	208.36	855	0.34	2.71	56.72
6.139	6.994	132.89	1.72	23.33	1.762	5	88	213.34	870	0.92	3.95	60.67
6.297	7.167	136.17	2.85	26.18	1.805	10	98	220.84	889	0.00		60.67
6.389	7.278	138.28	2.40	28.58	1.851	5	103	230.49	903	1.80	3.79	64.46

| 6.543 | 7.446 | 141.47 | 2.17 | 30.75 | 1.971 | 4 | 107 | 252.76 | 960 | 0.80 | 2.55 | 67.01 |

ACKNOWLEDGEMENTS

CONFLICTS OF INTEREST

The authors declare that they have no conflicts of interest.

REFERENCES

[1]	XU Renping, WANG Shuliang, YE Yong (2006) Monitoring of Highway Soft Soil Road Bed Stability. Technology of Highway and Transport (4): 9-13.

[2]	RAO Bo, WEI Limin (2005) A Stability Control Method for Fill Embankment on Soft Ground. Journal of Highway and Transportation Research and Development 22(2):46-49.

[3]	LI Yuanming (2004) Stability Evaluation during Staged Construction of Embankment. Nanjing: Southeast University.

[4]	TAVENAS F, MIEUSSENS C, BOURGES F (1979) Lateral Displacement in Clay Foundation under Embankments. Canadian Geotechnical Journal (16): 532-550.

[5]	BRAND Edward, BRENNER R.P (1981) Soft Clay Engineering. Elserier scientific publishing company, Amsterdam.

[6]	LADD C.C (1991) Stability Evaluation during Staged Construction: 22nd Terzaghi Lecture. Journal of Geotechnical Engineer, ASCE 117(4): 537-615.

[7]	TAVENAS F, et al (1978) The Stability of Stage-constructed Embankments on Soft Clays. Can. Geotech (15): 285-305.

[8]	ZHOU Jing (1999) Settlement Analysis of Embankment on Soft Clay. China Railway Science 20(2): 17-29.

[9]	LIU Zengxian, TANG Liansheng. (2003) Analysis on Lateral Squeeze Settlement of Soft Clay Foundation under Embankment. Geotechnical Investigation and Surveying (2): 1-4.

[10]	LI Fei, CHENG Penghuan, SHAN Haiyin, et al (2004) Testing Study on Lateral Deformation of Soft Road Ground and its Control.Chinese Journal of Rock Mechanics and Engineering 23(12):2114-2117.

[11]	HUANG Teng, TAN Xiangshao, WU Yugang (2007) A Practical Stability Analysis Method for the Soft Soil Foundation on Pearl River Delta. Chinese Journal of Geotechnical Engineering 29(3): 391-397.

[12]	WANG Yanling, CHEN Jianfeng (2002) Monitoring Methods of High Filled Road Bed in Soft Soil Areas. Journal of Engineering Geology 10(S1): 668-671.

[13]	WANG Yanhui (2016) Stability Judgment of Soft Soil Subgrade in Mountainous Area based on AGO Method. Highway Traffic Technology (Applied Technology Edition) (7):104-106.

[14]	HUANG Teng, WU Yugang (2005) A Method for Stability Analysis of Soft Subgrade Based on Measured Settlement Data. The Proceeding of National Symposium on Expressway Foundation Treatment 49-56.

[15]	Fellenius W (1927) Earth Stability Calculations Assuming Friction and Cohesion on Circular Slip Surfaces. Ernst, Berlin.

[16]	WANG Yongping, ZHANG Gongxin, ZENG Qingjun, et al (2005) Determination of Loading Plan Using Thin-Layer Rotary Adding Method. Port & Waterway Engineering (9): 62-64,100.

[17]	Ministry of Housing and Urban-Rural Development of the People's Republic of China (2012) Technical Code for Ground Treatment of Buildings (JGJ 79-2012), Beijing: China Building Industry Press.

[18]	XIE Chuang (2015) Stability Control Method of Highway Soft Soil Foundation Treatment Construction. Theoretical Research in Urban Construction 5(3): 489-490.